

# The F-box protein RCN127 enhances rice tillering and grain yield by mediating the degradation of OsTB1 and OsTCP19

Rong Miao<sup>1,†</sup>, Xin Wang<sup>2,†</sup>, Miao Feng<sup>2,†</sup>, Zhijun Cheng<sup>2</sup>, Jiale Shao<sup>2</sup>, Chunlei Zhou<sup>2</sup>, Jinsheng Qian<sup>2</sup>, Yajing Luo<sup>2</sup>, Wenfan Luo<sup>2</sup>, Sheng Luo<sup>2</sup>, Bin Lei<sup>2</sup>, Xin Liu<sup>2</sup>, Shuai Li<sup>2</sup>, Yimin Ling<sup>2</sup>, Jian Wang<sup>2</sup>, Tong Luo<sup>2</sup>, Yulong Ren<sup>2</sup>, Cailin Lei<sup>2</sup> , Shanshan Zhu<sup>2</sup>, Zhichao Zhao<sup>2</sup>, Ling Jiang<sup>1,3,\*</sup>, Qibing Lin<sup>2,\*</sup> and Jianmin Wan<sup>1,2,3,\*</sup> 

<sup>1</sup>National Key Laboratory of Crop Genetics & Germplasm Enhancement and Utilization, Jiangsu Nanjing National Field Scientific Observation and Research Station for Rice Germplasm, Nanjing Agricultural University, Nanjing, China

<sup>2</sup>State Key Laboratory of Crop Gene Resource and Breeding, Institute of Crop Science, Chinese Academy of Agricultural Sciences, Beijing, China

<sup>3</sup>Zhongshan Biological Breeding Laboratory, Nanjing, China

Received 21 April 2025;

revised 21 May 2025;

accepted 22 May 2025.

\*Correspondence (Tel 13002575525; fax 025-84399061; email [jiangling@njau.edu.cn](mailto:jiangling@njau.edu.cn) (L.J.), Tel 15010751286; fax 82105837; email [lingqibing@caas.cn](mailto:lingqibing@caas.cn) (Q.L.), Tel 13601466713; fax 025-84396516; email [wanjm@njau.edu.cn](mailto:wanjm@njau.edu.cn) (J.W.))

<sup>†</sup>These authors contributed equally to this work.

## Summary

Tillering ability is a crucial agronomic trait that determines rice yield potential. OsTB1 (the rice ortholog of TEOSINTE BRANCHED 1) and OsTCP19 of the TCP protein family are two key repressors of rice tillering. Until now, their post-translational regulatory mechanisms have remained elusive. In this study, we identified the F-box protein RCN127 as a novel post-translational regulator that promotes rice tillering by targeting them for degradation. The *rcn127* mutant exhibits reduced tillering. The target gene *RCN127* encodes an F-box protein that localizes in both the nucleus and cytoplasm, with higher expression levels in roots, stem bases, and young panicles. We demonstrate that RCN127 physically interacts with both OsTB1 and OsTCP19, mediating their ubiquitination and subsequent degradation via the 26S proteasome pathway. This reduction in OsTB1 and OsTCP19 protein levels weakens their suppression on tillering, leading to significantly increased tiller numbers. Importantly, RCN127-mediated regulation enhances grain yield in both the model variety Nipponbare and the dominant cultivated variety LJ31, providing a promising strategy for yield improvement. Therefore, our study unveils a novel post-translational regulatory mechanism of TCP protein family, providing a new strategy to increase grain yield by enhancing rice tillering capacity.

**Keywords:** rice (*Oryza sativa* L.), *RCN127*, tillering, grain yield, *OsTB1*, *OsTCP19*.

## Introduction

Rice (*Oryza sativa* L.) is one of the world's most vital staple crops, and enhancing its yield is a powerful strategy to alleviate food shortages driven by the rapidly increasing global population (Khush, 1997). Panicle number, grains per panicle, and grain weight are the three key agronomic traits that fundamentally determine grain yield potential. Among the three factors, panicle number is predominantly governed by rice tillering capacity – the plant's inherent ability to generate productive tillers. Additionally, rice tillering capacity is a key determinant of plant architecture (Wang et al., 2018; Wang and Li, 2008; Xing and Zhang, 2010). Several genetic pathways involved in the regulation of rice tillering (plant branching) have been identified, including the *MONOCULM1* (*MOC1/LS/LAS*) pathway (Greb et al., 2003; Li et al., 2003; Lin et al., 2020; Schumacher et al., 1999; Shao et al., 2019), *REGULATOR OF AXILLARY MERISTEMS* (*BLIND/RAX*) pathway (Guo et al., 2015; Keller et al., 2006; Müller et al., 2006), *LAX PANICLE* (*LAX/BA1*) pathway (Komatsu et al., 2001, 2003; Oikawa and Kyojuka, 2009; Tabuchi et al., 2011), *TEOSINTE BRANCHED 1* (*TB1/FC1/BRC1*) pathway (Doebley et al., 1997; Kumar et al., 2021; Minakuchi et al., 2010), and the Strigolactone (SL) signalling pathway (Duan et al., 2019; Fang

et al., 2020; Gomez-Roldan et al., 2008; Hu et al., 2024; Jiang et al., 2013; Umehara et al., 2008; Zhou et al., 2013, 2025).

Among these pathways, the *TB1/FC1/BRC1* pathway is a crucial genetic pathway regulating the ability of plant branching (rice tillering). Studies have shown that genes within this pathway, including *TB1*, *OsTB1* (*FC1*), *BRC1*, *PsBRC1*, and *SIBRC1*, suppress branching in various plants such as maize, rice, Arabidopsis, pea, and tomato. Among these genes, *TB1* plays a pivotal role in the domestication of maize, transforming it from a multi-stalked plant into a single-stalked plant (Aguilar-Martínez et al., 2007; Braun et al., 2012; Doebley et al., 1997; Martín-Trillo et al., 2011; Minakuchi et al., 2010). This pathway is regulated by SL and other plant hormones. In rice, mutations within the microRNA miR156 binding site of *SQUAMOSA PROMOTER BINDING PROTEIN-LIKE 14* (*SPL14*) disrupt miR156-mediated degradation of *SPL14* mRNA, resulting in a marked upregulation of *SPL14* expression. The elevated *SPL14* expression triggers pronounced suppression of rice tillering (Jiao et al., 2010). Further research revealed that *SPL14* interacts with DWARF53 (D53), a suppressor of the SL pathway, to antagonistically regulate the *TB1/FC1/BRC1* pathway (Lu et al., 2013; Song et al., 2017). Meanwhile, SL and brassinosteroid (BR) antagonistically regulate the stability of the D53-BRASSINAZOLE-RESISTANT1 (*OsBZR1*) complex to determine

Please cite this article as: Miao, R., Wang, X., Feng, M., Cheng, Z., Shao, J., Zhou, C., Qian, J., Luo, Y., Luo, W., Luo, S., Lei, B., Liu, X., Li, S., Ling, Y., Wang, J., Luo, T., Ren, Y., Lei, C., Zhu, S., Zhao, Z., Jiang, L., Lin, Q. and Wan, J. (2025) The F-box protein RCN127 enhances rice tillering and grain yield by mediating the degradation of OsTB1 and OsTCP19. *Plant Biotechnol. J.*, <https://doi.org/10.1111/pbi.70180>.

the expression of *FC1* during rice tillering (Fang et al., 2020). Additionally, *OstB1* interacts with MADS-box transcription factor *OsMADS57*, attenuating the transcriptional repression of *DWARF14 (D14)* by *OsMADS57*, thus repressing rice tillering (Guo et al., 2013).

Rice tillering is closely related to environmental growth conditions. High levels of fertilizer, water, and high light intensity promote tillering, while low levels of fertilizer, water, and low light intensity inhibit plant growth and branching (rice tillering) (Shen et al., 2013). NITROGEN-MEDIATED TILLER GROWTH RESPONSE 5 (*NGR5*) interacts with DELLA proteins, which competitively bind to the gibberellin receptor *GA-INSENSITIVE DWARF 1 (GID1)*, inhibiting gibberellin-mediated degradation of *NGR5*. This enhances the stability of *NGR5*, thereby increasing rice tiller number and promoting nitrogen uptake and utilization (Wu et al., 2020). The TCP family member *OstTCP19* suppresses rice tillering by downregulating the expression of the tillering-promoting gene *DWARF AND LOW-TILLERING (DLT)*. When a 29-base pair fragment is inserted into the promoter of *OstTCP19*, its expression is downregulated, leading to enhanced nitrogen use efficiency in rice varieties containing this variation (Liu et al., 2021).

The *OstTCP19* and the genes in the *TB1/FC1/BRC1* pathway are classified to the TCP gene family (Martín-Trillo and Cubas, 2010). Previous studies demonstrated that the TCP genes are transcriptionally regulated by environmental factors and plant hormones (Yu et al., 2022), and negatively regulated by microRNAs such as *miR319* and *miR164* (Lan and Qin, 2020). However, the regulatory mechanisms at the post-translational level, particularly at the protein level, remain poorly understood.

In this study, we identified a positive regulatory gene for rice tillering, *RCN127*, which encodes a protein containing an F-box domain and belongs to a class of F-box proteins exclusive to monocot plants. We found that *RCN127* can interact with *OstB1* and *OstTCP19* to ubiquitinate and degrade *OstB1* and *OstTCP19* proteins through the proteasome pathway, thereby increasing tiller number and rice yield. Therefore, our study uncovers a key regulatory mechanism governing TCP genes at the post-translational level, offering a novel strategy to enhance rice yield through optimized tillering control.

## Results

### *RCN127* positively regulates rice tillering

To investigate the new regulatory mechanisms of rice tillering, we obtained a *reduced culm number127-1 (rcn127-1)* mutant from a knockout mutant library in Nipponbare (NIP) background. We found that the *rcn127-1* mutant was caused by the mutation of *Os04g0313500*, and obtained two knockout lines (*rcn127-1* and *rcn127-2*). Phenotypic analysis revealed that both lines exhibited reduced plant height and tiller number (Figure 1a–c; Figure S1). Additionally, panicle length, secondary branch number, grain number per panicle, seed setting rate, and flag leaf length were significantly reduced, while primary branch number and flag leaf width showed no significant differences (Table S1). Furthermore, we measured the seedling length of wild-type (WT) (Nipponbare) and *rcn127-1* mutant plants grown hydroponically for 4 weeks and found that the seedling length of the *rcn127-1* mutant was significantly shorter than that of the WT (Figure 1d,e). We also analysed the panicle length and internode length of WT and *rcn127-1* mutant plants, revealing that the panicle length and internode length of the *rcn127-1* mutant were significantly

shorter than those of the WT (Figure 1f,g), indicating that the reduced plant height in the *rcn127-1* mutant is attributed to the decreased panicle length and internode length. Moreover, we performed a genome complementation of the *rcn127-1* mutant, resulting in three independent lines. These lines showed effective restoration of plant height and tillering number (Figure S2). These findings demonstrate that the mutation in the *RCN127* leads to a dwarf and low-tillering phenotype, indicating that the *RCN127* is a positive regulator of rice tillering.

### Subcellular localization and expression pattern of *RCN127*

The expression pattern of *RCN127* in different organs and panicles with different lengths (reflecting different developmental stages) was detected using RT-qPCR. The results indicated that *RCN127* was highly expressed in roots and shoot bases, and lowly expressed in young panicles. With the elongation of the young panicle, the expression level of *RCN127* increased gradually (Figure S3a). mRNA *in situ* hybridization showed that *RCN127* was strongly expressed in tiller bud (Figure S3b). To determine the subcellular localization of *RCN127*, the full-length coding sequence of *RCN127* was fused to the N-terminus and C-terminus of green fluorescent protein (GFP), respectively. When transiently expressed in rice protoplasts, the GFP signal was clearly observed in both the nucleus and the cytoplasm, suggesting that *RCN127* is a nuclear and cytoplasmic localized protein (Figure S3c).

Analysis of the NCBI database revealed that *RCN127* contains an F-box domain at its N-terminus (Figure S4a). Phylogenetic analysis further indicated that *RCN127* belongs to a class of genes exclusive to monocots (Figure S4b). To confirm whether *RCN127* is an F-box protein, we identified *OSK* genes as the rice homologues of the Arabidopsis gene *ASK1* (Figure S5a). Yeast two-hybrid assays demonstrated that *RCN127* interacted with *OSK1* and *OSK8*, and these interactions were further confirmed by co-immunoprecipitation (Co-IP) assays, respectively (Figure S5b–d). These results indicate that *RCN127* is an F-box protein.

### *RCN127* interacts with *OstB1* and promotes its degradation

To identify the substrate protein of *RCN127*, we screened a yeast library and identified *OstB1* as a possible interacting protein of *RCN127*. The interaction between *RCN127* and *OstB1* was confirmed by an *in vivo* co-immunoprecipitation (Co-IP) assay and a bimolecular fluorescence complementation (BiFC) assay in rice protoplasts (Figure 2a,b). We conducted a series of biochemical experiments to test whether *RCN127* mediates the degradation of *OstB1*. The *in vitro* ubiquitination assay demonstrated that the total protein extracts from WT plants polyubiquitinated more *OstB1* proteins, whereas extracts from *rcn127-1* mutant plants polyubiquitinated fewer *OstB1* proteins (Figure 2c), indicating that *RCN127* is involved in the ubiquitination of *OstB1*. Cell-free degradation assays indicated that the purified recombinant MBP–*OstB1*–His protein was degraded faster using total protein extracts from WT plants than by those from *rcn127-1* mutant plants. MG132, a specific inhibitor of the 26S proteasome, evidently blocked the degradation of MBP–*OstB1*–His protein in both total protein extracts (Figure 2d). Additionally, the protein level of *OstB1* was higher in the *rcn127-1* mutant and lower in *RCN127* overexpressing lines compared with WT plants (Figure 2e), suggesting that *RCN127* promotes the degradation

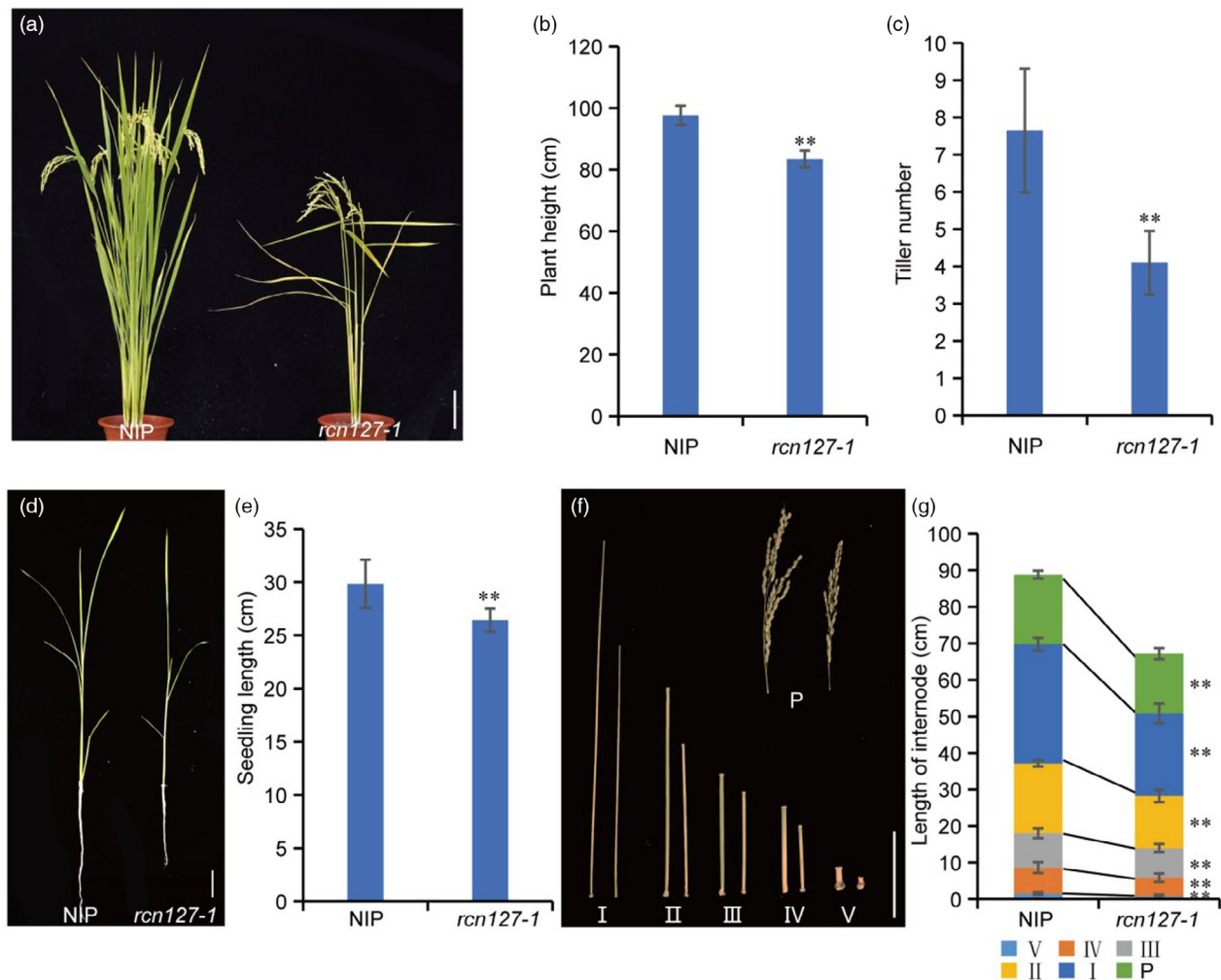


**Figure 1** Phenotypes of the wild-type (WT) and *rcn127-1* mutant. (a) Plant phenotypes of WT and *rcn127-1* mutant at the mature stage. Bar, 5 cm. (b, c) The plant height (b) and tiller number (c) of WT and *rcn127-1* mutant at the mature stage. Values are means  $\pm$  SD,  $n = 20$ . (d, e) Plant phenotypes (d) and seedling length (e) of WT and *rcn127-1* mutant observed after 4-week hydroponic cultivation. Values are means  $\pm$  SD of 15 plants. Bar, 2 cm. (f) Panicle and internode morphological characteristics of the WT and *rcn127-1* mutant. P denotes the panicle; I to V label internodes from top to bottom. Bar, 10 cm. (g) Panicle and internode length of the WT and *rcn127-1* mutant. Values are means  $\pm$  SD,  $n = 15$ . \*\* $P < 0.01$ , Student's *t*-test.

of OsTB1 via the proteasome pathway in *planta*. To further validate the regulatory relationship between *RCN127* and *OsTB1*, we generated a double mutant of *rcn127-1* and *ostb1* (Figure 2f; Figure S6a). Phenotypic analysis showed that the double mutant exhibited similar plant height and tiller number to those of the *ostb1* single mutant (Figure 2g,h), indicating that *OsTB1* acts downstream of *RCN127* genetically.

### RCN127 interacts with OsTCP19 and promotes its degradation

Based on a previous study (Liu *et al.*, 2021), we found that another TCP transcription factor, OsTCP19, also negatively regulates rice tillering. To explore whether OsTCP19 is another downstream target of RCN127 in tillering regulation, we conducted further analyses. Co-IP and BiFC assays confirmed the interaction between RCN127 and OsTCP19 (Figure 3a,b). *In vitro* ubiquitination assays showed that OsTCP19 was polyubiquitinated at a slower rate by total protein extracts from *rcn127-1* mutant plants compared with those from WT plants (Figure 3c). Additionally, cell-free degradation assays revealed that purified

recombinant GST–OsTCP19 protein was degraded more rapidly by total protein extracts from WT plants than by those from *rcn127-1* mutant plants. Moreover, MG132 evidently blocked the GST–OsTCP19 degradation in both extracts (Figure 3d). Furthermore, the protein level of OsTCP19 was higher in *rcn127-1* mutant but lower in *RCN127*-overexpressing lines compared with WT plants (Figure 3e), indicating that RCN127 regulates the degradation of OsTCP19 via the proteasome pathway in *planta*. To further validate the regulatory relationship between *RCN127* and *OsTCP19*, we generated a double mutant of *rcn127-1* and *ostcp19* (Figure 3f; Figure S6b). Phenotypic analysis showed that the double mutant exhibited similar plant height and tiller number to those of the *ostcp19* single mutant (Figure 3g,h), suggesting that *OsTCP19* acts downstream of *RCN127* genetically.

### RCN127 exhibits functional redundancy with its homologous protein RCN128

Through NCBI BLAST analysis, we identified 12 homologous genes of *RCN127* in rice and found that RCN127 shares the

## 4 Rong Miao et al.

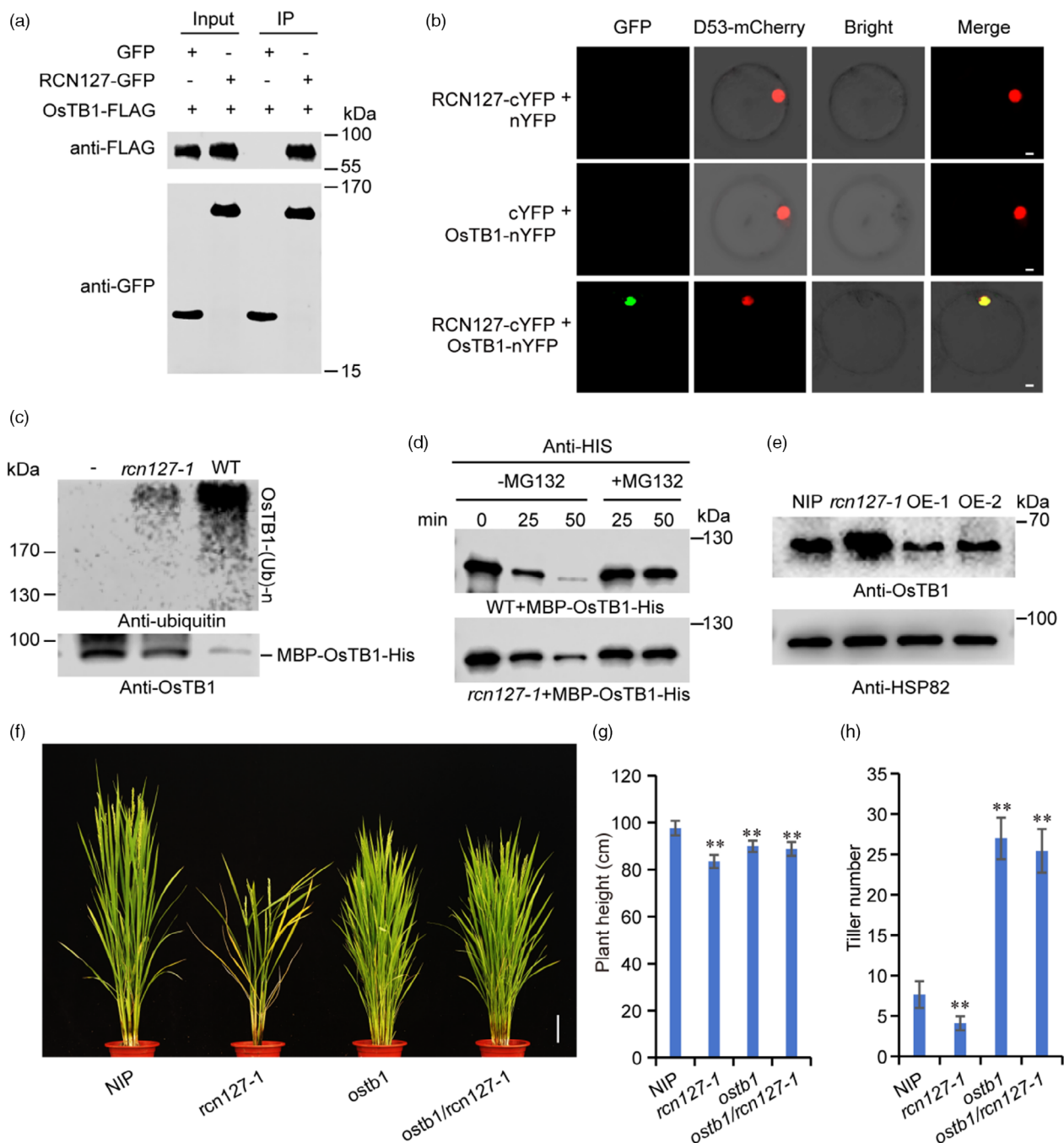


**Figure 2** RCN127 promotes OsTB1 protein degradation. (a) Co-IP assay reveals the interaction between RCN127 and OsTB1 in rice protoplasts. GFP beads were used in the immunoprecipitation assay. Immunoblots were probed with anti-Flag or anti-GFP antibody. (b) Bimolecular fluorescence complementation (BiFC) assays show that RCN127 interacts with OsTB1 in rice protoplasts. RCN127-cYFP was co-expressed with OsTB1-nYFP in rice protoplasts. D53-mCherry was used as a nuclear marker. (c) *In vitro* ubiquitination assay shows that more OsTB1 proteins are ubiquitinated by WT plant extracts than by *rcn127-1* mutant plant extracts. (d) Cell-free degradation assay shows the stability of MBP-OsTB1-His protein in WT and *rcn127-1* mutant plant extracts with or without 40  $\mu$ M proteasome inhibitor MG132, respectively. (e) Immunoblot assay shows the levels of OsTB1 protein in the shoot bases of WT, *rcn127-1* mutant, and RCN127 overexpression lines (OE-1 and OE-2). "Anti-HSP82" indicates that roughly equal amounts of total plant extracts were used. (f) Morphologies of NIP, *rcn127-1*, *ostb1*, and *ostb1/rcn127-1* double mutant. Bar, 10 cm. (g, h) Statistical analysis of plant height (g) and tiller number (h) across NIP, *rcn127-1*, *ostb1*, and *ostb1/rcn127-1* double mutant. Values are means  $\pm$  SD,  $n = 20$ . \*\* $P < 0.01$ , Student's *t*-test.

highest protein homology (90.71%) with RCN128 (an F-box protein) (Figure 4a,b). We generated two knockout lines of RCN128 (Figure S7). Compared with the WT, the two *rcn128* mutants exhibited reduced plant height and a comparable tiller number (Figure 4c-e). We also generated a double mutant by

knocking out RCN128 in the *rcn127-1* mutant background. The double mutant plants showed significantly reduced plant height and tiller number compared with the *rcn127-1* single mutant (Figure 4f-h; Figure S8). These results suggest that RCN127 and RCN128 share partially redundant functions.

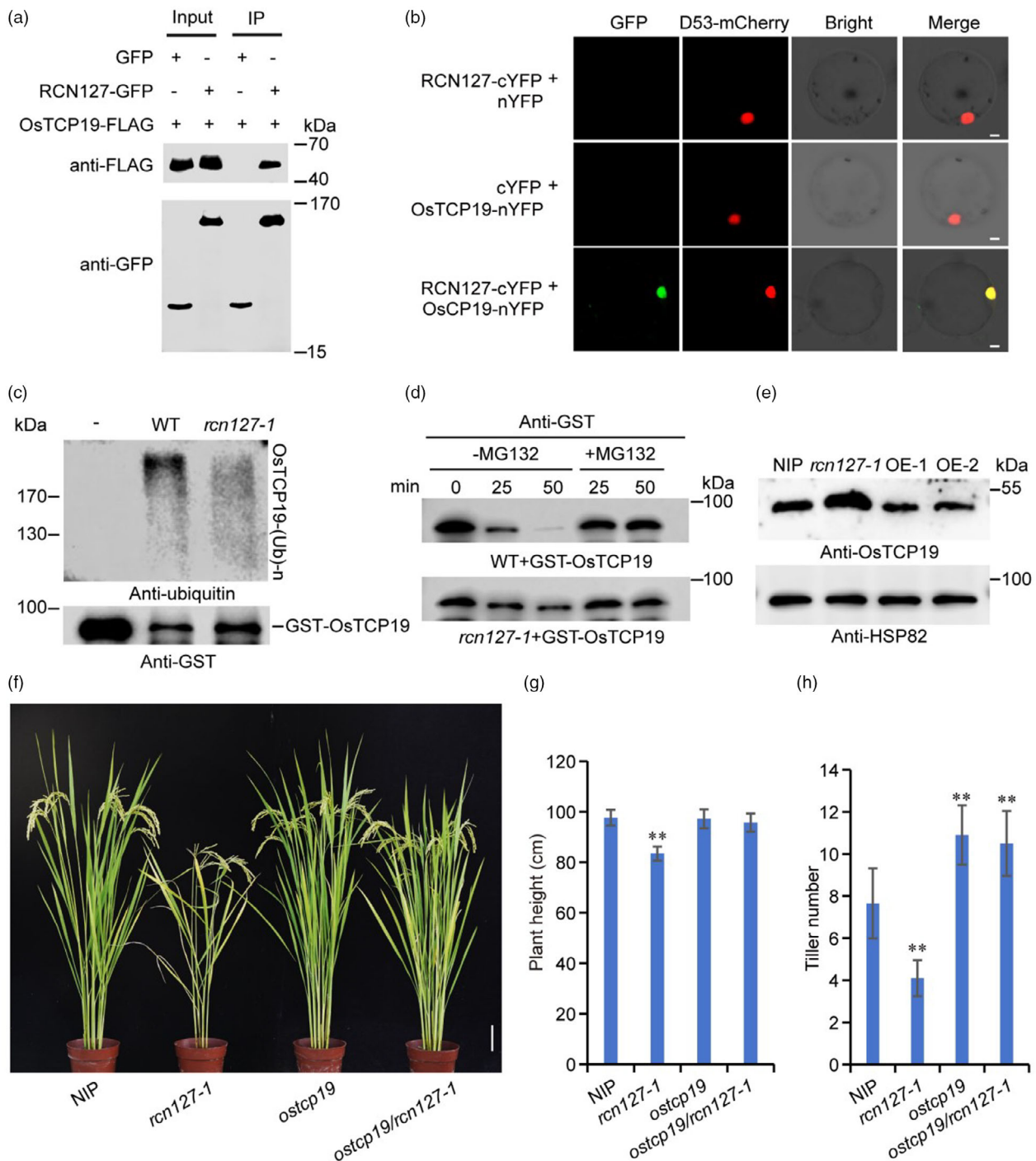


**Figure 3** RCN127 also promotes OsTCP19 protein degradation. (a) Co-IP assay shows the interaction between RCN127 and OsTCP19 in rice protoplasts. GFP beads were used in the immunoprecipitation assay. Immunoblots were probed with anti-Flag or anti-GFP antibody. (b) BiFC assays show that RCN127 interacts with OsTCP19 in rice protoplasts. RCN127-cYFP was co-expressed with OsTCP19-nYFP in rice protoplasts. D53-mCherry was used as a nuclear marker. Bar, 5 μm. (c) *In vitro* ubiquitination assay shows that more OsTCP19 proteins are ubiquitinated by WT plant extracts than by *rcn127-1* mutant plant extracts. (d) Cell-free degradation assay shows the stability of GST-OsTCP19 protein in WT and *rcn127-1* mutant plant extracts with or without 40 μM proteasome inhibitor MG132, respectively. (e) Immunoblot assay shows the levels of OsTCP19 protein in the shoot bases of WT, *rcn127-1* mutant and RCN127 overexpression lines (OE-1 and OE-2). "Anti-HSP82" indicates that roughly equal amounts of total plant extracts were used. (f) Morphologies of NIP, *rcn127-1*, *ostcp19*, and *ostcp19/rcn127-1* double mutant. Bar, 10 cm. (g, h) Statistical analysis of plant height (g) and tiller number (h) of NIP, *rcn127-1*, *ostcp19*, and *ostcp19/rcn127-1* double mutant. Values are means ± SD, n = 20. \*\*P < 0.01, Student's t-test.

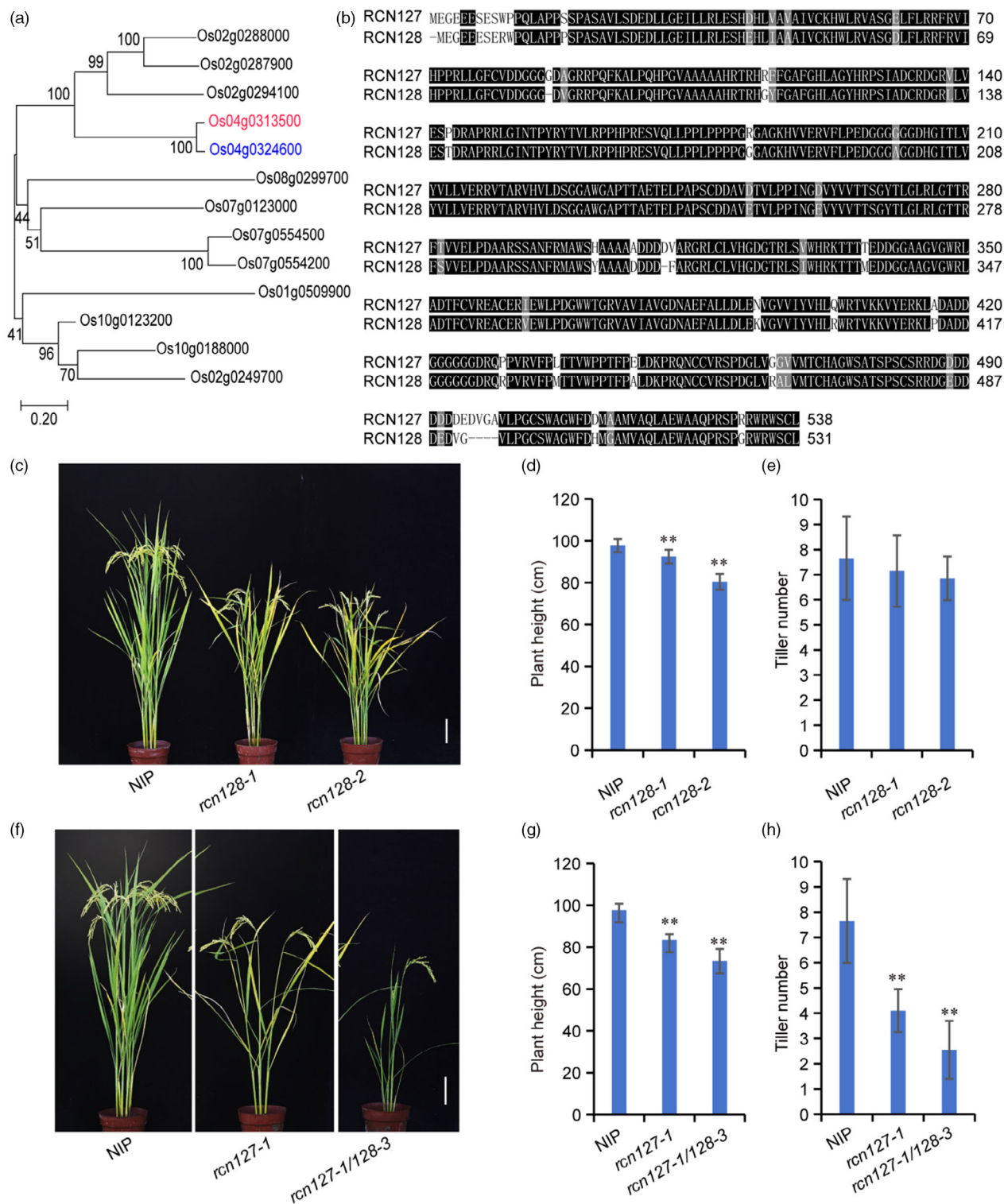


**Figure 4** RCN127 and RCN128 exhibit functional redundancy. (a) Phylogenetic analysis of the RCN127 protein and its homologues. The red gene is RCN127, while the blue gene is RCN128. (b) Homologous protein alignment between RCN127 and RCN128. (c) Morphologies of NIP, *rcn128-1*, and *rcn128-2* mutants. Bar, 10 cm. (d, e) Statistical analysis of plant height (d) and tiller number (e) of NIP, *rcn128-1*, and *rcn128-2* mutants. Values are means  $\pm$  SD,  $n = 20$ . (f) Morphologies of NIP, *rcn127-1*, and *rcn127-1/rcn128-3* double mutant. Bar, 10 cm. (g, h) Statistical analysis of plant height (g) and tiller number (h) of NIP, *rcn127-1*, and *rcn127-1/rcn128-3* double mutant. Values are means  $\pm$  SD,  $n = 20$ . \*\* $P < 0.01$ , Student's  $t$ -test.

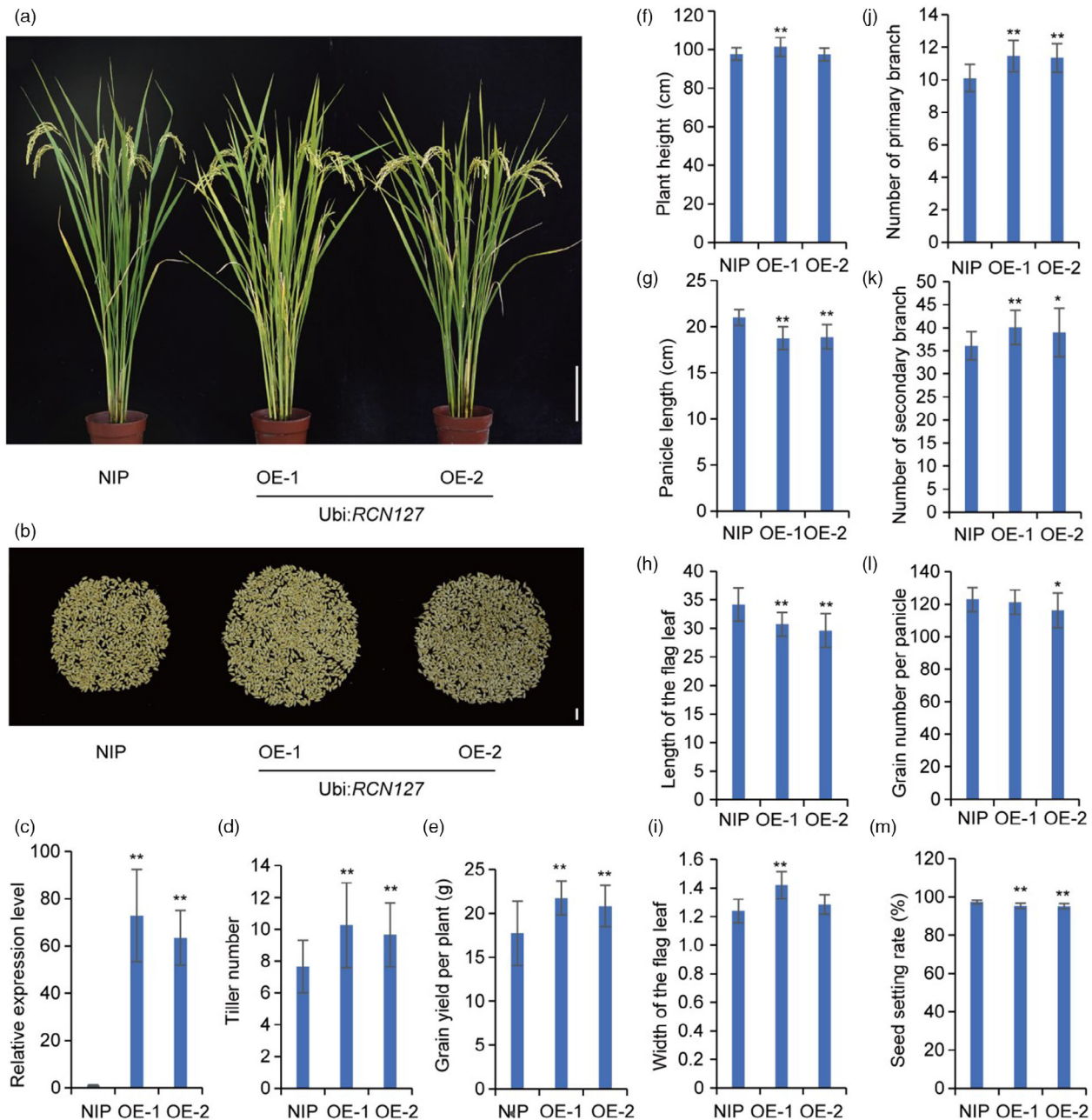


**Figure 5** Phenotypes of transgenic plants overexpressing *RCN127*. (a) Morphologies of NIP and its *RCN127* overexpression lines (OE-1 and OE-2) under the control of the Ubi promoter. Bar, 10 cm. (b) Grain yield per plant of NIP and *RCN127* overexpression lines (OE-1 and OE-2). Bar, 1 cm. (c) RT-qPCR analysis of *RCN127* expression in NIP and two OE lines. Values are means  $\pm$  SD,  $n = 3$ . (d–m) Statistics of tiller number (d), grain yield per plant (e), plant height (f), panicle length (g), length of the flag leaf (h), width of the flag leaf (i), number of primary branch (j), number of secondary branch (k), grain number per panicle (l), seed setting rate (m). Values are means  $\pm$  SD,  $n = 20$ . \* $P < 0.05$ ; \*\* $P < 0.01$  determined by Student's *t*-test.

### Overexpression of *RCN127* increases tiller number and yield per plant

To evaluate the potential of *RCN127* in rice breeding, the full coding sequence of *RCN127* driven by the Ubi promoter was introduced into the NIP variety. Two positive overexpression lines (OE-1, OE-2) showed significantly higher expression levels than the WT, and the tiller number also increased evidently (Figure 5a, c, d). Meanwhile, the yield per plant increased by 22.8% and 17.6%, respectively (Figure 5b, e). Additionally, plant height was slightly increased (Figure 5f). Compared with the WT, panicle

length, flag leaf length, and seed setting rate were slightly reduced (Figure 5g, h, m), while flag leaf width, primary branches, and secondary branches significantly increased (Figure 5i–k). However, there was no significant difference in grain number per panicle (Figure 5l). These results demonstrate that overexpression of *RCN127* significantly increases tiller number, thereby enhancing yield per plant.

Furthermore, the full coding sequence of *RCN127* driven by the 35S promoter was introduced into the NIP variety. Two positive overexpression lines (OX-1, OX-2) exhibited significantly higher expression levels and increased tiller number than the WT

(Figure S9a,c,d). Meanwhile, the yield per plant increased by 17.3% and 13.3%, respectively (Figure S9b,e). Panicle length, flag leaf length, and seed setting rate were reduced in the two overexpression lines (Figure S9g,h,m), while flag leaf width and primary branches were increased notably (Figure S9i,j). No significant differences were observed in plant height, secondary branch number, and grain number per panicle (Figure S9f,k,l). These results further demonstrate that overexpression of *RCN127* significantly increases tiller number, thereby enhancing yield per plant.

To validate the yield-enhancing potential of *RCN127* in other varieties, the full coding sequence of *RCN127* driven by the Ubi promoter was introduced into the Longjing 31 (LJ31), a major variety cultivated in Northeast China. Two positive overexpression lines (OE-1, OE-2) showed significantly higher expression levels than the WT, and the tiller number also increased notably (Figure S10a,c,d). Meanwhile, the yield per plant increased by 20% and 23% compared with the WT plants, respectively (Figure S10b,e). Plant height, flag leaf length, and seed setting rate were reduced in the overexpression lines (Figure S10f,h,m). Panicle length, secondary branch number, and grain number per panicle were increased in the OE-2 line but not in the OE-1 line (Figure S10g,k,l), while no significant differences were observed in flag leaf width or primary branch number of both lines (Figure S10i,j).

To understand the evolution of the *RCN127* gene among the subspecies of rice, we analysed the polymorphism of *RCN127* in the RiceVarMap v2.0 dataset and then detected two major haplotypes of *RCN127* (Figure S11a) using nine single-nucleotide polymorphisms (SNPs) in the coding sequence (CDS) region (rare haplotypes of <100 accessions are not shown). The two haplotypes displayed significant differentiation between *Xian* and *Geng* (Figure S11a,b), with Hap1 predominantly found in *Geng* and Hap2 mainly present in *Xian*. However, no significant difference in tiller number was observed between Hap1 and Hap2 (Figure S11c). Additionally, we found that rice varieties carrying Hap1 are primarily cultivated in China (Figure S11d), while those with Hap2 are mainly grown in South Asia, South Africa, and South America (Figure S11e).

In summary, we identified a novel tillering-promoting gene in rice, *RCN127*, which increases tiller number to enhance rice yield by mediating the degradation of OsTB1 and OsTCP19 through the 26S proteasome pathway (Figure 6).

## Discussion

Rice tillers are developed from axillary buds in the leaf axils and are generally considered a key factor controlling grain yield (Wang and Li, 2011). TCP proteins are characterized by a highly conserved ~60-amino acid TCP domain in their N-terminal region, which contains an atypical basic helix-loop-helix (bHLH) motif for DNA binding and protein-protein interactions (Cubas et al., 1999; Li, 2015). Based on amino acid sequence differences, TCP proteins are classified into two categories: Class I and Class II (Viola et al., 2023). Class I TCP proteins possess a shorter TCP domain, lacking four amino acid residues compared with that of Class II TCPs (Lan and Qin, 2020). Class II TCPs are further divided into two subclasses: CYC/TB1-like TCP (CYC/TB1) and CININNATA-like TCP (CIN) (Martín-Trillo and Cubas, 2010). In the genes regulating rice tillering, *OsTCP19* is classified within the Class I TCP subfamily and plays a relatively weak role in repressing rice tillering, whereas *OsTB1* of the *TB1/FC1/BRC1* pathway

belongs to the Class II TCP subfamily and plays a strong role in repressing rice tillering (Yang et al., 2018; Yao et al., 2007). At the transcriptional level, SL and BR antagonistically regulate the stability of the D53-OsBZR1 complex to determine the expression of *FC1* (*OsTB1*) during rice tillering (Fang et al., 2020; Takeda et al., 2003). Nitrogen-induced lateral organ boundaries domain (LBD) proteins OsLBD37 and OsLBD39 efficiently bind to the *OsTCP19* promoter, inhibiting its activity and consequently promoting rice tillering (Liu et al., 2021). At the post-transcriptional level, the expression of TCP genes including *OsTB1* and *OsTCP19* is likely regulated by conserved microRNAs miR319 and miR164 (Lan and Qin, 2020; Yu et al., 2022). However, the protein-level regulatory mechanism of TCP proteins remains elusive. In this study, we identified a mutant with reduced tillers caused by the mutation of *RCN127*. *RCN127* encodes an F-box subunit of the SCF E3 ligase complex, which is expressed at high levels in roots and stem bases, and localized to the nucleus and cytoplasm (Figure 1; Figure S3). Furthermore, *RCN127* interacts with *OsTB1* and *OsTCP19* respectively, promoting their ubiquitination and degradation through the 26S proteasome pathway. These processes consequently reduce the protein levels of *OsTB1* and *OsTCP19*, thereby promoting rice tillering (Figures 2 and 3). Therefore, our study reveals a novel post-translational mechanism of the TCP genes.

Plant F-box proteins, involved in a series of biological processes, are typically categorized into three classes (FBWs, FBLs, FBXs) according to their C-terminal domain (Craig, 1999; Nguyen and Busino, 2020). *RCN127*, which lacks a recognizable C-terminal domain, is classified as an FBXs-type F-box protein (Figure S4a). Among *RCN127* homologues in rice, *RCN128* exhibits the highest homology at 90.71% (Figure 4a, b). The double mutant of *RCN128* and *RCN127* exhibited shorter plant height and reduced tiller number compared with the *rcn127-1* single mutant (Figure 4c-h), demonstrating the partial functional redundancy between *RCN127* and *RCN128* (Figure 4c-h). Notably, *RCN127* and *RCN128* are F-box proteins exclusive to monocot plants (Figure S4). The TCP proteins, crucial in plant growth and development in both monocots and dicots (Carrara and Dornelas, 2021; Challa et al., 2021; Fang et al., 2024; Martín-Trillo and Cubas, 2010; Qin et al., 2022; Tao et al., 2013), raise the interesting question of whether there is a specific class of F-box proteins that regulate the ubiquitination and degradation of TCP proteins in dicots. The panicle number is one of the three key factors determining crop yield, and it is closely linked to the number of tillers produced by the plant (Xing and Zhang, 2010). To investigate the potential applications of *RCN127*, we overexpressed *RCN127* in both the NIP and LJ31 backgrounds. In the NIP background, overexpression of *RCN127* driven by both Ubi and 35S promoter resulted in a significant increase in tiller number and yield per plant (Figure 5; Figure S9). In the Longjing 31, a dominant variety that is widely cultivated in Northeast China, overexpression lines of *RCN127* driven by the Ubi promoter also exhibited a significant increase in tiller number and yield per plant (Figure S10).

Notably, our findings demonstrate that in the NIP genetic background, transgenic plants overexpressing *RCN127* under either the Ubi or 35S promoter exhibited consistent phenotypic alterations, including shortened panicle length and reduced seed setting rates (Figure 5g,m; Figure S9g,m). However, distinct agronomic traits were observed in the LJ31 background, where *RCN127* overexpression lines showed significantly increased panicle length, reduced plant height, and unchanged primary

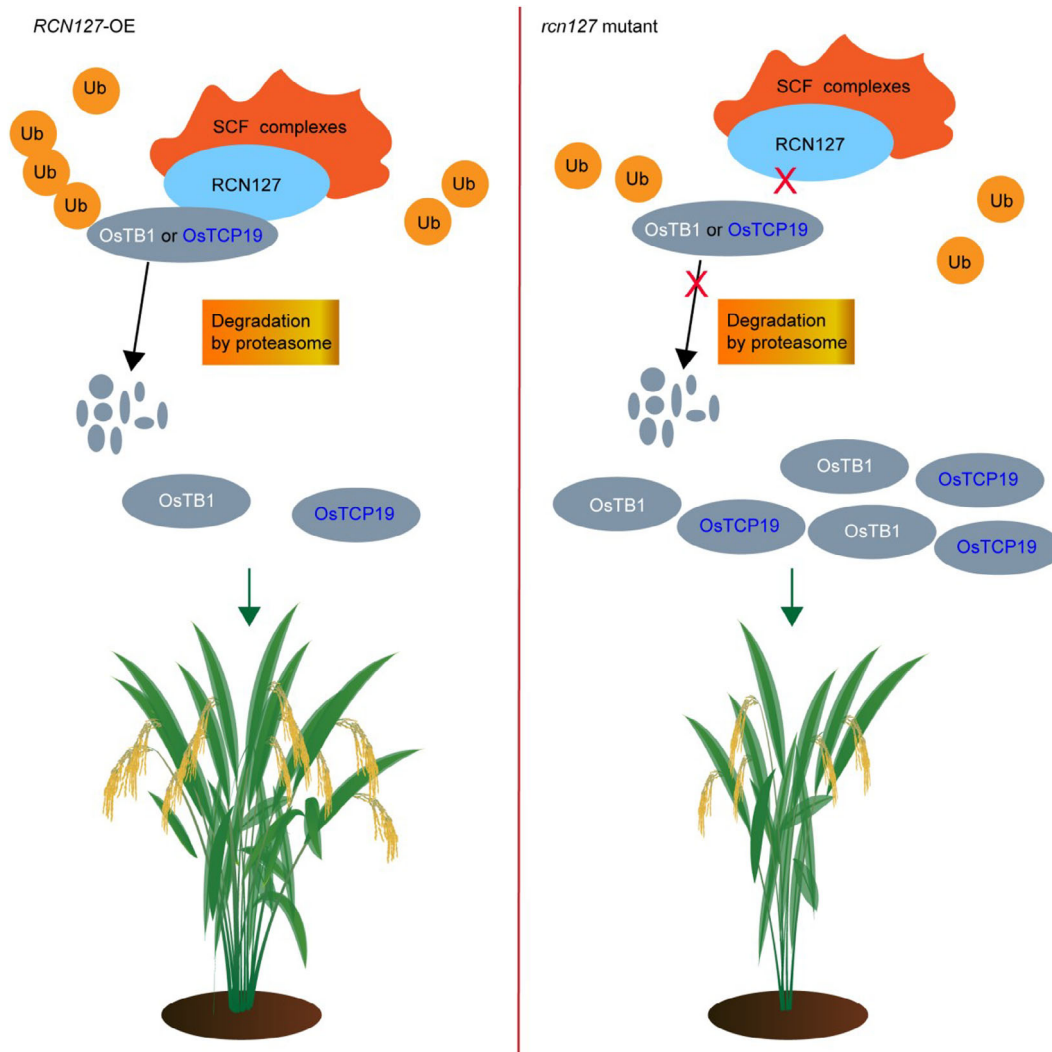


**Figure 6** A proposed model of RCN127 increasing the grain yield by promoting rice tillering. RCN127 interacts with OsTB1 and OsTCP19 and then promotes their degradation via the 26S proteasome system, resulting in the improvement of grain yield by promoting rice tillering. In the *rcn127* mutant, OsTB1 and OsTCP19 accumulate due to the absence of RCN127-mediated degradation, thereby repressing rice tillering and the grain yield of the *rcn127* mutant.

branch number (Figure S10f,g,j). In NIP plants, while the reduction in panicle length and fertility would theoretically undermine yield potential, this effect might be partially counterbalanced by the increased primary and secondary branches (Figure 5j,k; Figure S9j). These cultivar-dependent phenotypic variations suggest that *RCN127* consistently promotes tiller formation but functions differentially in regulating other agronomic traits in different genetic backgrounds of rice.

Therefore, these findings demonstrate that RCN127 acts as a positive regulator in promoting rice tillering, and upregulating its expression holds promising potential for increasing both panicle number and yield by enhancing rice tillering capacity.

## Experimental procedures

### Plant materials and growing conditions

To produce *RCN127* CRISPR-Cas9 knockout lines, we designed 18 bp sgRNA targeting sites (*RCN127*-Crispr-F/R) on the exons of

*RCN127* and introduced them into NIP. To knock out the *RCN128*, *OsTB1*, and *OsTCP19* genes, the specific gRNA for each target gene was designed through the CRISPR-P website (<http://crispr.hzau.edu.cn/CRISPR2/>). The genome sequence of *RCN127* was amplified using primers 2300-*RCN127*-F/R and inserted into the 2300 vector to generate a transformation plasmid with an In-Fusion Advantage Cloning Kit (Clontech, Beijing, China), and the construct was introduced into the *rcn127-1* mutant by *Agrobacterium tumefaciens*-mediated transformation. Primers 1305-*RCN127*-F/R and pCUBi1390-*RCN127*-F/R were used to amplify the CDS sequence of *RCN127*, and the PCR product was inserted into the 1305 and pCUBi1390 vector to generate a transformation plasmid using an In-Fusion Advantage Cloning Kit (Clontech), respectively, and the construct was introduced into NIP by *Agrobacterium tumefaciens*-mediated transformation. All plants were grown in a paddy field at the Shunyi Experimental Station of the Institute of Crop Science, Chinese Academy of Agricultural Sciences located at Beijing.

### RNA extraction and RT-qPCR analysis

RNA was extracted following the instructions of the Quick-RNA™ Plant Miniprep Kit (Zymo Research, California, USA). First-strand cDNA was synthesized from 1 µg total RNA using the PrimeScript 1<sup>st</sup> Strand cDNA Synthesis Kit (Tiangen, Beijing, China). Real-time quantitative PCR (RT-qPCR) of various genes was performed on an ABI Prism 7500 Real-Time PCR System using the TB Green Premix Ex Taq™ Kit (Takara, Shiga, Japan) according to the manufacturer's instructions. The rice house-keeping gene *UBQ* (*Os03g0234200*) served as the reference gene. The quantitative primers used in this study are listed in Table S2.

### In situ RNA hybridization

RNA *in situ* hybridization was performed as described (Bradley *et al.*, 1993). A 157 bp coding region of *RCN127* was cloned into the pGEM-T Easy vector (Promega, Wisconsin, USA) and used as a template to generate antisense and sense RNA probes. The basal stems of rice seedlings at the third and fourth leaf stages were fixed in formaldehyde–acetic acid–ethanol (FAA, RNase-free) solution. DIG-labelled RNA probes were prepared following the manufacturer's instructions (DIG Northern Starter Kit, Cat. No. 2039672, Roche, Basel, Switzerland). Slides were observed under bright-field microscopy using a Leica DM5000 (B) microscope.

### Subcellular localization

A 1617-bp coding sequence of *RCN127* was amplified with primers RCN127-PAN580GFP-F/R, and the PCR product was inserted into the XbaI/BamHI sites in the PAN580-GFP vector driven by the CaMV35S promoter, resulting in the RCN127-GFP fusion protein-expressing plasmid, which was then transformed into rice protoplasts grown from 11-day-old seedlings, and incubated at 24 °C for 24 h in darkness before examination. The D53-mCherry plasmid was used as a control. Similarly, the CDS coding sequence of *RCN127* was amplified with primers PAN580GFP-RCN127-F/R, and the PCR product was inserted into the BglII/PstI sites of the PAN580-GFP vector driven by the CaMV35S promoter. This plasmid and the D53-mCherry plasmid were co-transformed. GFP fluorescence was observed after 24 h using a confocal laser scanning microscope (LSM 980; Zeiss, Baden-Württemberg, Germany).

### Phylogenetic analysis

About 28 homologous protein sequences of RCN127 were downloaded from the NCBI website (<http://blast.ncbi.nlm.nih.gov/Blast.cgi>). The Clustal program was used for multiple alignment of amino acid sequences, and a phylogenetic tree was constructed using Mega software (MEGA X), and the bootstrap test was conducted with 1000 replicates.

### Bimolecular fluorescence complementation (BiFC) assay

The full-length cDNA of RCN127 was amplified and inserted into cYFP (C-terminal end of yellow fluorescent protein (YFP)) via the BamHI and Sall sites, and the full-length cDNAs of OsTB1 and OsTCP19 were amplified and inserted into nYFP (N-terminal end of YFP) via the BamHI and Sall sites, respectively. Then co-transferred RCN127 and OsTB1, as well as RCN127 and OsTCP19 into rice protoplasts, respectively. GFP fluorescence was observed after 20 h using a confocal laser scanning microscope (LSM 980; Zeiss, Baden-Württemberg, Germany).

### Co-immunoprecipitation (Co-IP) assays

The coding sequences of *RCN127*, *OSK8*, and *OSK1* were cloned into Flag and GFP tagging plasmids, respectively. The coding sequences of *OsTB1* and *OsTCP19* were cloned into a Flag tagging plasmid. Each fusion construct was transiently co-expressed in rice protoplasts, and samples were extracted with 500 µL of protein extraction solution (0.5 M sucrose, 50 mM Tris–HCl (pH 8.0), 5 mM DTT, 1 mM MgCl<sub>2</sub>, 10 mM EDTA, and 1× incubation mixture of protease inhibitors) and incubated at 4 °C for 12 min, then centrifuged at 15 871 *g* for 10 min and collected the supernatant. Ten µL GFP beads were added to the supernatant and incubated for 50 min. Beads were collected and washed five times with protein washing solution. Then, 1× Protein Loading Buffer and the GFP beads were mixed at 100 °C for 10 min. The proteins were separated by 10% SDS-PAGE and detected by immunoblotting with anti-Flag (M185-7; Medical & Biological Laboratories (MBL), Tokyo, Japan) and anti-GFP (PMO13-7; MBL, Tokyo, Japan) antibodies.

### In vitro ubiquitination assay

Purified MBP–OsTB1–His protein bound to Amylose Resin (NEB) was incubated at 28 °C with an equal amount of crude extract from rice seedlings in a buffer (25 mM Tris–HCl pH 7.5, 10 mM MgCl<sub>2</sub>, 5 mM dithiothreitol, 10 mM NaCl, 10 mM ATP, and 50 µM MG132). After incubation for the specified time at 28 °C according to the manufacturer's instructions, the MBP–OsTB1–His and MBP–OsTB1–His–(Ub)<sub>n</sub> fusion proteins were cleaved by Factor Xa (NEB) at room temperature. The supernatant containing OsTB1 or OsTB1–(Ub)<sub>n</sub> was mixed with SDS-PAGE loading buffer and then loaded onto an SDS-PAGE gel. Western blotting was performed using anti-OsTB1 antibody or anti-polyubiquitin antibody (Beijing Protein Innovation, <http://www.proteomics.org.cn/>) at a dilution of 1:1000. HRP-conjugated anti-rabbit IgG (H + L) (1:5000 dilution, MBL, Tokyo, Japan) was used as the secondary antibody. The Western blot was developed using ECL reagent (GE Healthcare, Chicago, IL, USA). Similarly, purified GST–OsTCP19 protein bound to BeaverBeads (GSH) was incubated at 28 °C with an equal amount of crude extract from rice seedlings in a buffer. The next experimental steps were similar to OsTB1, and the ubiquitination level of GST–OsTCP19 was detected finally with anti-GST or anti-polyubiquitin antibodies.

### Cell-free degradation assays

*In vitro* protein stability assay was performed as described previously (Fu *et al.*, 2012). The MBP–OsTB1–His or GST–OsTCP19 fusion proteins were expressed in the *E. coli* strain BL21 and purified. The total proteins of *rcn127* mutant and NIP plants were subsequently extracted using degradation buffer (25 mM Tris–HCl (pH 7.0), 10 mM MgCl<sub>2</sub>, 10 mM NaCl, and 5 mM DTT) and mixed with the same amount of purified MBP–OsTB1–His or GST–OsTCP19 protein, and then 10 mM ATP was added to the reaction mixture. Samples were collected at the indicated times and subjected to immunoblotting with an anti-His or anti-GST antibody.

### Accession numbers

Sequence data from this article can be found in the GenBank/EMBL data libraries under the following accession numbers: *RCN127*, *Os04g0313500*; *RCN128*, *Os04g0324600*; *OsTB1*, *Os03g0706500*; *OsTCP19*, *Os06g0226700*; *UBQ*, *Os03g0234200*.

## Acknowledgements

This research was supported by grants from Biological Breeding-National Science and Technology Major Project (2024ZD04077, 2023ZD04072), the National Key Research and Development Programme of China (2022YFD1200104), the Special Modern Agricultural Foundation of Jiangsu Key R&D project (Grant No. BE2023362), Innovation Programme of Chinese Academy of Agricultural Sciences (CAAS-CSCB-202401), Central Public-interest Scientific Institution Basal Research Fund (No. Y2024YJ13), and the National Natural Science Foundation of China (31671769). It was also supported by the Key Laboratory of Biology, Genetics, and Breeding of Japonica Rice in Mid-lower Yangtze River, Ministry of Agriculture, China, Jiangsu Collaborative Innovation Centre for Modern Crop Production, Jiangsu Nanjing National Observation and Research Station of Rice Germplasm Resources, and Southern Japonica Rice Research and Development Co. LTD.

## Conflict of interest

The authors declare no conflicts of interest.

## Author contributions

Jianmin Wan, Qibing Lin, and Ling Jiang supervised the project. Rong Miao, Xin Wang, and Miao Feng designed and performed most of the experiments. Zhijun Cheng provided theoretical guidance. Jiale Shao, Chunlei Zhou, Jinsheng Qian, Yajing Luo, Wenfan Luo, and Zhichao Zhao performed field work. Sheng Luo, Bin Lei, Xin Liu, Shuai Li, Yimin Ling, Jian Wang, Tong Luo, Yulong Ren, Cailin Lei, and Shanshan Zhu provided technical assistance. Rong Miao and Qibing Lin analysed data and wrote the manuscript. Jianmin Wan, Qibing Lin, and Ling Jiang revised the manuscript. All authors read and approved this manuscript.

## Data availability statement

The data that support the findings of this study are available in the supplementary material of this article.

## References

Aguilar-Martínez, J.A., Poza-Carrión, C. and Cubas, P. (2007) Arabidopsis BRANCHED1 acts as an integrator of branching signals within axillary buds. *Plant Cell* **19**, 458–472.

Bradley, D., Carpenter, R., Sommer, H., Hartley, N. and Coen, E. (1993) Complementary floral homeotic phenotypes result from opposite orientations of a transposon at the plena locus of *antirrhinum*. *Cell* **72**, 85–95.

Braun, N., de Saint Germain, A., Pillot, J.P., Boutet-Mercey, S., Dalmais, M., Antoniadi, I., Li, X. *et al.* (2012) The pea TCP transcription factor PsBRC1 acts downstream of Strigolactones to control shoot branching. *Plant Physiol.* **158**, 225–238.

Carrara, S. and Dornelas, M.C. (2021) TCP genes and the orchestration of plant architecture. *Trop Plant Biol* **14**, 1–10.

Challa, K.R., Rath, M., Sharma, A.N., Bajpai, A.K., Davuluri, S., Acharya, K.K. and Nath, U. (2021) Active suppression of leaflet emergence as a mechanism of simple leaf development. *Nat Plants* **7**, 1264–1275.

Craig, K.L. (1999) The F-box: a new motif for ubiquitin dependent proteolysis in cell cycle regulation and signal transduction. *Prog. Biophys. Mol. Biol.* **72**, 299–328.

Cubas, P., Lauter, N., Doebley, J. and Coen, E. (1999) The TCP domain: a motif found in proteins regulating plant growth and development. *Plant J.* **18**, 215–222.

Doebley, J., Stec, A. and Hubbard, L. (1997) The evolution of apical dominance in maize. *Nature* **386**, 485–488.

Duan, J.B., Yu, H., Yuan, K., Liao, Z.G., Meng, X.B., Jing, Y.H., Liu, G.F. *et al.* (2019) Strigolactone promotes cytokinin degradation through transcriptional activation of *CYTOKININ OXIDASE/DEHYDROGENASE 9* in rice. *Proc. Natl. Acad. Sci. USA* **116**, 14319–14324.

Fang, Y.X., Guo, D.S., Wang, Y., Wang, N., Fang, X.W., Zhang, Y.H., Li, X. *et al.* (2024) Rice transcriptional repressor OsTIE1 controls anther dehiscence and male sterility by regulating JA biosynthesis. *Plant Cell* **36**, 1697–1717.

Fang, Z.M., Ji, Y.Y., Hu, J., Guo, R.K., Sun, S.Y. and Wang, X.L. (2020) Strigolactones and brassinosteroids antagonistically regulate the stability of the D53-OsBZR1 complex to determine FC1 expression in rice tillering. *Mol. Plant* **13**, 586–597.

Fu, Z.Q., Yan, S.P., Saleh, A., Wang, W., Ruble, J., Oka, N., Mohan, R. *et al.* (2012) NPR3 and NPR4 are receptors for the immune signal salicylic acid in plants. *Nature* **486**, 228–232.

Gomez-Roldan, V., Feras, S., Brewer, P.B., Puech-Pagès, V., Dun, E.A., Pillot, J.P., Letisse, F. *et al.* (2008) Strigolactone inhibition of shoot branching. *Nature* **455**, 189–194.

Greb, T., Clarenz, O., Schäfer, E., Müller, D., Herrero, R., Schmitz, G. and Theres, K. (2003) Molecular analysis of the LATERAL SUPPRESSOR gene in Arabidopsis reveals a conserved control mechanism for axillary meristem formation. *Genes Dev.* **17**, 1175–1187.

Guo, D.S., Zhang, J.Z., Wang, X.L., Han, X., Wei, B.Y., Wang, J.Q., Li, B.X. *et al.* (2015) The WRKY transcription factor WRKY71/EXB1 controls shoot branching by transcriptionally regulating RAX genes in Arabidopsis. *Plant Cell* **27**, 3112–3127.

Guo, S.Y., Xu, Y.Y., Liu, H.H., Mao, Z.W., Zhang, C., Ma, Y., Zhang, Q.R. *et al.* (2013) The interaction between OsMADS57 and OsTB1 modulates rice tillering via DWARF14. *Nat. Commun.* **4**, 1566.

Hu, Q.L., Liu, H.H., He, Y.J., Hao, Y.R., Yan, J.J., Liu, S.M., Huang, X.H. *et al.* (2024) Regulatory mechanisms of strigolactone perception in rice. *Cell* **187**, 7551–7567.

Jiang, L., Liu, X., Xiong, G.S., Liu, H.H., Chen, F.L., Wang, L., Meng, X.B. *et al.* (2013) DWARF 53 acts as a repressor of strigolactone signalling in rice. *Nature* **504**, 401–405.

Jiao, Y.Q., Wang, Y.H., Xue, D.W., Wang, J., Yan, M.X., Liu, G.F., Dong, G.J. *et al.* (2010) Regulation of SPL14 by OsmiR156 defines ideal plant architecture in rice. *Nat. Genet.* **42**, 541–544.

Keller, T., Abbott, J., Moritz, T. and Doerner, P. (2006) Arabidopsis REGULATOR OF AXILLARY MERISTEMS1 controls a leaf axil stem cell niche and modulates vegetative development. *Plant Cell* **18**, 598–611.

Khush, G.S. (1997) Origin, dispersal, cultivation and variation of rice. *Plant Mol. Biol.* **35**, 25–34.

Komatsu, K., Maekawa, M., Ujii, S., Satake, Y., Furutani, I., Okamoto, H., Shimamoto, K. *et al.* (2003) LAX and SPA: major regulators of shoot branching in rice. *Proc. Natl. Acad. Sci. USA* **100**, 11765–11770.

Komatsu, M., Maekawa, M., Shimamoto, K. and Kyojuka, J. (2001) The LAX1 and FRIZZY panicle 2 genes determine the inflorescence architecture of rice by controlling rachis-branch and spikelet development. *Dev. Biol.* **231**, 364–373.

Kumar, V., Kim, S.H., Adnan, M.R., Heo, J., Jeong, J.H., Priatama, R.A., Lee, J.J. *et al.* (2021) Tiller outgrowth in rice (*Oryza sativa* L.) is controlled by OsGT1, which acts downstream of FC1 in a *PhyB*-independent manner. *J. Plant Biol.* **64**, 417–430.

Lan, J.Q. and Qin, G.J. (2020) The regulation of CIN-like TCP transcription factors. *Int. J. Mol. Sci.* **21**, 4498.

Li, S. (2015) The Arabidopsis thaliana TCP transcription factors: a broadening horizon beyond development. *Plant Signal. Behav.* **10**, e1044192.

Li, X.Y., Qian, Q., Fu, Z.M., Wang, Y.H., Xiong, G.S., Zeng, D.L., Wang, X.Q. *et al.* (2003) Control of tillering in rice. *Nature* **422**, 618–621.

Lin, Q.B., Zhang, Z., Wu, F.Q., Feng, M., Sun, Y., Chen, W.W., Cheng, Z.J. *et al.* (2020) The APC/C<sup>TE</sup> E3 ubiquitin ligase complex mediates the antagonistic regulation of root growth and tillering by ABA and GA. *Plant Cell* **32**, 1973–1987.

- Liu, Y.Q., Wang, H.R., Jiang, Z.M., Wang, W., Xu, R.N., Wang, Q.H., Zhang, Z.H. *et al.* (2021) Genomic basis of geographical adaptation to soil nitrogen in rice. *Nature* **590**, 600–605.
- Lu, Z.F., Yu, H., Xiong, G.S., Wang, J., Jiao, Y.Q., Liu, G.F., Jing, Y.H. *et al.* (2013) Genome-wide binding analysis of the transcription activator ideal plant architecture1 reveals a complex network regulating rice plant architecture. *Plant Cell* **25**, 3743–3759.
- Martín-Trillo, M. and Cubas, P. (2010) TCP genes: a family snapshot ten years later. *Trends Plant Sci.* **15**, 31–39.
- Martín-Trillo, M., Grandio, E.G., Serra, F., Marcel, F., Rodríguez-Buey, M.L., Schmitz, G., Theres, K. *et al.* (2011) Role of tomato BRANCHED1-like genes in the control of shoot branching. *Plant J.* **67**, 701–714.
- Minakuchi, K., Kameoka, H., Yasuno, N., Umehara, M., Luo, L., Kobayashi, K., Hanada, A. *et al.* (2010) FINE CULM1 (FC1) works downstream of strigolactones to inhibit the outgrowth of axillary buds in rice. *Plant Cell Physiol.* **51**, 1127–1135.
- Müller, D., Schmitz, G. and Theres, K. (2006) Blind homologous R2R3 Myb genes control the pattern of lateral meristem initiation in Arabidopsis. *Plant Cell* **18**, 586–597.
- Nguyen, K.M. and Busino, L. (2020) The biology of F-box proteins: The SCF family of E3 ubiquitin ligases. *Adv. Exp. Med. Biol.* **1217**, 111–122.
- Oikawa, T. and Kyoizuka, J. (2009) Two-step regulation of LAX PANICLE1 protein accumulation in axillary meristem formation in rice. *Plant Cell* **21**, 1095–1108.
- Qin, W.Q., Wang, N., Yin, Q., Li, H.L., Wu, A.M. and Qin, G.J. (2022) Activation tagging identifies WRKY14 as a repressor of plant thermomorphogenesis in Arabidopsis. *Mol. Plant* **15**, 1725–1743.
- Schumacher, K., Schmitt, T., Rossberg, M., Schmitz, C. and Theres, K. (1999) The Lateral suppressor (Ls) gene of tomato encodes a new member of the VHLID protein family. *P. Natl. Acad. Sci. USA* **96**, 290–295.
- Shao, G., Lu, Z., Xiong, J., Wang, B., Jing, Y., Meng, X., Liu, G. *et al.* (2019) Tiller bud formation regulators MOC1 and MOC3 cooperatively promote tiller bud outgrowth by activating *FON1* expression in rice. *Mol. Plant* **12**, 1090–1102.
- Shen, J.B., Li, C.J., Mi, G.H., Li, L., Yuan, L.X., Jiang, R.F. and Zhang, F.S. (2013) Maximizing root/rhizosphere efficiency to improve crop productivity and nutrient use efficiency in intensive agriculture of China. *J. Exp. Bot.* **64**, 1181–1192.
- Song, X.G., Lu, Z.F., Yu, H., Shao, G.N., Xiong, J.S., Meng, X.B., Jing, Y.H. *et al.* (2017) IPA1 functions as a downstream transcription factor repressed by D53 in strigolactone signaling in rice. *Cell Res.* **27**, 1128–1141.
- Tabuchi, H., Zhang, Y., Hattori, S., Omae, M., Shimizu-Sato, S., Oikawa, T., Qian, Q. *et al.* (2011) LAX PANICLE2 of rice encodes a novel nuclear protein and regulates the formation of axillary meristems. *Plant Cell* **23**, 3276–3287.
- Takeda, T., Suwa, Y., Suzuki, M., Kitano, H., Ueguchi-Tanaka, M., Ashikari, M., Matsuoka, M. *et al.* (2003) The *OsTB1* gene negatively regulates lateral branching in rice. *Plant J.* **33**, 513–520.
- Tao, Q., Guo, D.S., Wei, B.Y., Zhang, F., Pang, C.X., Jiang, H., Zhang, J.Z. *et al.* (2013) The TIE1 transcriptional repressor links TCP transcription factors with TOPLESS/TOPLESS-RELATED corepressors and modulates leaf development in Arabidopsis. *Plant Cell* **25**, 421–437.
- Umehara, M., Hanada, A., Yoshida, S., Akiyama, K., Arite, T., Takeda-Kamiya, N., Magome, H. *et al.* (2008) Inhibition of shoot branching by new terpenoid plant hormones. *Nature* **455**, 195–200.
- Viola, I.L., Alem, A.L., Jure, R.M. and Gonzalez, D.H. (2023) Physiological roles and mechanisms of action of class I TCP transcription factors. *Int. J. Mol. Sci.* **24**, 5437.
- Wang, B., Smith, S.M. and Li, J.Y. (2018) Genetic regulation of shoot architecture. *Annu. Rev. Plant Biol.* **69**, 437–468.
- Wang, Y. and Li, J. (2011) Branching in rice. *Curr. Opin. Plant Biol.* **14**, 94–99.
- Wang, Y.H. and Li, J.Y. (2008) Molecular basis of plant architecture. *Annu. Rev. Plant Biol.* **59**, 253–279.
- Wu, K., Wang, S.S., Song, W.Z., Zhang, J.Q., Wang, Y., Liu, Q., Yu, J.P. *et al.* (2020) Enhanced sustainable green revolution yield via nitrogen-responsive chromatin modulation in rice. *Science* **367**, 641.
- Xing, Y.Z. and Zhang, Q.F. (2010) Genetic and molecular bases of rice yield. *Annu. Rev. Plant Biol.* **61**, 421–442.
- Yang, Y., Nicolas, M., Zhang, J.Z., Yu, H., Guo, D.S., Yuan, R.R., Zhang, T.T. *et al.* (2018) The TIE1 transcriptional repressor controls shoot branching by directly repressing BRANCHED1 in Arabidopsis. *PLoS Genet.* **14**, e1007296.
- Yao, X., Ma, H., Wang, J. and Zhang, D.B. (2007) Genome-wide comparative analysis and expression pattern of TCP gene families in *Arabidopsis thaliana* and *Oryza sativa*. *J. Integr. Plant Biol.* **49**, 885–897.
- Yu, L., Chen, Q.W., Zheng, J.R., Xu, F., Ye, J.B., Zhang, W.W., Liao, Y.L. *et al.* (2022) Genome-wide identification and expression pattern analysis of the TCP transcription factor family in *Ginkgo biloba*. *Plant Signal. Behav.* **17**, 1994248.
- Zhou, A., Kane, A., Wu, S., Wang, K., Santiago, M., Ishiguro, Y., Yoneyama, K. *et al.* (2025) Evolution of interorganismal strigolactone biosynthesis in seed plants. *Science* **387**, eadp0779.
- Zhou, F., Lin, Q.B., Zhu, L.H., Ren, Y.L., Zhou, K.N., Shabek, N., Wu, F.Q. *et al.* (2013) D14-SCF(D3)-dependent degradation of D53 regulates strigolactone signalling. *Nature* **532**, 406–410.

## Supporting information

Additional supporting information may be found online in the Supporting Information section at the end of the article.

**Figure S1** Identification of *Os04g0313500* knockout mutants generated by CRISPR/Cas9 in variety NIP.

**Figure S2** Complementation of the *rcn127-1* mutation.

**Figure S3** Subcellular localization and expression pattern of the *RCN127* gene.

**Figure S4** The phylogenetic analysis of *RCN127* protein.

**Figure S5** *RCN127* interacts with OSKs.

**Figure S6** The genotype of *OsTB1* or *OsTCP19* editing line.

**Figure S7** The genotypes of *rcn128-1* and *rcn128-2* editing lines.

**Figure S8** The genotype of *RCN128* in *rcn127-1/rcn128-3* double mutant.

**Figure S9** Phenotypes of transgenic plants overexpressing *RCN127* under the control of the 35S promoter.

**Figure S10** Phenotypes of transgenic plants overexpressing *RCN127* in LJ31.

**Figure S11** Genetic diversity of *RCN127* in the RiceVarMap v2.0 dataset and Rice 3K dataset.

**Table S1** Agronomic traits of WT and *rcn127-1* mutant.

**Table S2** Primers used in this work.